Korean J. Chem. Eng., **27**(1), 104-109 (2010)
DOI: 10.1007/s11814-009-0312-6

Physical degradation of MEA in PEM fuel cell by on/off operation under nitrogen atmosphere

Dongho Seo*, Sangsun Park*, Yukwon Jeon*, Sung-Won Choi*, and Yong-Gun Shul*,,†**

*Department of Chemical and Biomolecular Engineering,
**The Specialized Graduate School of Hydrogen & Fuel Cell,
Yonsei University, 134 Shinchon-dong, Seodaemun-gu, Seoul 120-749, Korea
(*Received 12 May 2009 • accepted 23 June 2009*)

Abstract−The durability of PEMFCs is one of the most important issues for application in automotive vehicles with a repeated start-up and shut-down system. The understanding of degradation phenomena such as causes, mechanisms and influence of working condition is essential to improving the performance and lifetime of PEMFC. We conducted on/off cyclic operation in a single cell configuration with ultra purity nitrogen gas to investigate the physical degradation of membrane electrode assembly (MEA). After on/off cycle operation for 100,000 cycles under different humid condition, the characteristics of the MEAs were examined by in situ and ex situ analyses techniques. The physical degradation of MEA by on/off cycling led to a change in the membrane-electrode interfacial structure, which is mainly attributed to the loss of cell performance.

Key words: PEMFC, MEA Degradation, On/Off Cycle, Accelerated Stress Test

INTRODUCTION

Proton exchange membrane fuel cells (PEMFCs) have received considerable attention as a sustainable and eco-friendly energy conversion device for stationary and mobile applications. In recent years, the long-term durability of PEMFC has been one of the most important issues for commercial applications especially in automotive vehicles with a repeated start-up and shut-down system. The understanding of degradation phenomena such as causes, mechanism and influence of working condition is essential to improving the performance and lifetime of PEMFC. A variety of studies with regard to life cycle assessments of PEMFC system have been reported in the literature [1,2]. Many articles in these activities have dealt with degradation of the membrane electrode assembly (MEA) concerning severe working conditions such as insufficient reactant flows, high or low humidification of the reactant gases, high or low operating temperature and cycled operation [3-6].

Degradation of electrode including the growth, migration, contamination of platinum particles and corrosion of the carbon support lead to loss of electrocatalyst area [7-9]. Borup et al. reported that the rate of Pt particle growth occurs more rapidly during cycling to high potentials and with high relative humidity [10]. It is suggested that water molecules are able to penetrate between the metal islands and the substrate to lower the metal/substrate bonding energy, and consequently facilitate migration of the catalysts. On the other hand, carbon corrosion is found to increase with increasing temperature and decreasing relative humidity [10]. The degradation of carbon support is related to almost the oxidation of carbon. The reaction of carbon oxidation is often observed in an electrochemical system, according to $C+H_2O \rightarrow CO_2+4H^++4e^-$ at 0.207 V [11]. Carbon corrosion leads to a loss and change in structure of electrode, which forces catalytic metal nanoparticles to fall off the carbon support and decrease in the gas permeability and the electric contact with the current collector [12,13].

Membrane failure occurs in many forms including cracks, tears, punctures or pinholes. Non-uniform pressure during fuel cell operation can accelerate membrane degradation [14]. Inadequate humidification is detrimental to the membrane, as lack of water makes the membrane brittle and fragile. Liu et al. demonstrated that hydrogen crossover increased dramatically after 500 h of current cycling due to pinhole formation in the membrane [4]. Fluoride emission rate (FER) is used as an indicator of the membrane degradation rate [15]. The formation of hydroxyl (HO•) and hydroperoxyl (HOO•) radicals has been recognized as a source of chemical degradation of membrane. These radical species formed from H_2O_2 decomposition chemically attack the polymer at the endgroup sites, resulting in the ionomer damage and loss of PEM functionality and integrity [16]. In the long-term operation of a fuel cell, penetration of the catalyst particles into the membrane could be also observed, which may be the cause of local high stress areas [17].

Several accelerated degradation tests are proposed and implemented to estimate the performance and durability of the PEM fuel cell [18]. A fuel cell is a complex system with multi-interfaces between each of the components such as electrocatalysts, membrane, and gas diffusion media. Therefore, various interaction mechanisms during operation may contribute to loss of performance and negatively impact fuel cell durability. In this study, we focused on physical degradation of MEA by on/off cyclic operations with N_2/N_2. Also, the effect of different humid conditions of RH 80% and RH 50% on the physical degradation was discussed.

EXPERIMENTAL

Experiments were conducted in a single cell configuration with

†To whom correspondence should be addressed.
E-mail: shulyg@yonsei.ac.kr

commercial MEA (active area of 25 cm^2), teflon gaskets and graphite bipolar blocks with parallel serpentine channels. Carbon paper was used as the gas diffusion media and the Pt loadings of both anode and cathode were 0.4 mg/cm^2. Cartridge heaters were inserted into the end plates to control the cell temperature.

All the MEAs were activated with H_2/air at 70 °C cell temperature under relative humidity (RH) 100% overnight until stable cell voltage was observed. The hydrogen and air were passed through humidifiers prior to feeding into the fuel cell. Fig. 1 shows a schematic diagram of the experimental setup for on/off cyclic test. For on/off operations, all of the anode and cathode gas flows were switched to ultrapure nitrogen (99.9999%) and the flow rates of anode and cathode were 200 sccm and 500 sccm. The operation pressures at anode and cathode were 1.0 atm and 2.0 atm to enhance the physical degradation of MEA during on/off operation for 100,000 cycles under different humid condition of 80% and 50%, respectively. The cell pressure profile for on/off cycles in this study consisted of two steps, as shown in Fig. 2. In first step (θ_1), while nitrogen was supplied to the anode and the cathode for 9 sec, the outlet valves of anode and cathode were closed for 9 sec. In step 2 (θ_2), all of the inlet and outlet valves were opened for 1 sec. The maximum cell pressures (P_{cell}) of anode and cathode were observed at 0.8 atm and 1.9 atm during on/off cycles, respectively.

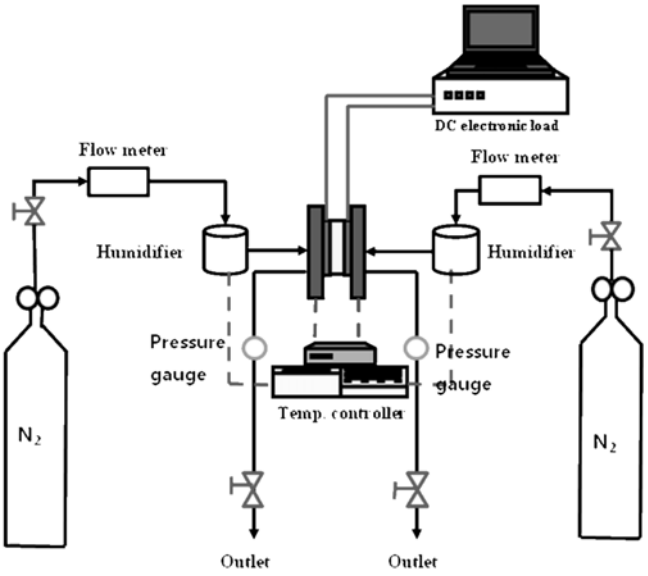

Fig. 1. Schematic diagram of experimental setup for outlet on/off cyclic operation.

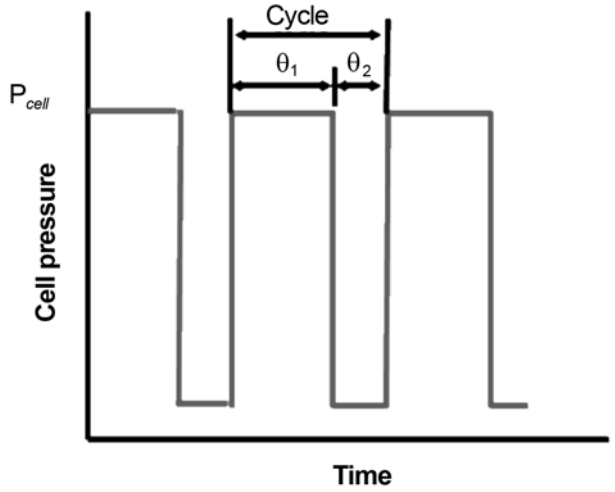

Fig. 2. The cell pressure profiles for the on/off cycles in this study. In step 1 (θ_1), inlet valves of anode and cathode were open but outlet valves of those closed for 9 sec. In step 2 (θ_2), inlet and outlet valves of anode and cathode were open for 1 sec. The maximum cell pressures (P_{cell}) of anode and cathode were observed at 0.8 atm and 1.9 atm during on/off cycles, respectively.

Both in situ and ex situ analyses techniques were carried out to diagnose the MEA degradation. I-V characteristic for MEA was evaluated by an electric load (Agilent 6060B) with H_2/air at 70 °C under relative humidity of 100%. Ohmic resistance and polarization resistance were estimated by measuring ac impedance using Autolab PGSTAT-30 in the frequency range from 10 kHz to 100 mHz. Cyclic voltammetry (CV) and linear sweep voltammetry (LSV) were used to determine electrochemical area (ECA) and hydrogen crossover current. In these methods, hydrogen with flow rate of 200 sccm and nitrogen with flow rate of 200 sccm are passed over the anode and cathode, respectively. The anode is used as the reference and counter electrode, and the cathode is used as the working electrode. The ex situ characterization of MEAs before and after on/off cyclic operation was carried out by X-ray diffraction (XRD) and energy dispersive X-ray spectroscopy (EDX). X-ray diffraction patterns for catalysts were obtained with a Rigaku Miniplex system using Cu Ka radiation between 20 and 80°. EDX measurements (Nissei Sangyo Co. Ltd, Hitachi model S-4200) were used to assign the Pt line scanning in the cross-section of MEAs. The cross-section of the MEAs was prepared by epoxy resin impregnation and ultramicrotome sectioning using a diamond knife.

RESULTS AND DISCUSSION

Fig. 3 shows the fuel cell performance curves for the MEAs before and after on/off operation for 100,000 cycles under different humid condition of RH 80% and RH 50%. Similar performance drops of two humid conditions are observed at high current density above 0.8 A/cm^2. The performance curve is divided into regimes where one of the processes of activation kinetics, ohmic resistance, or mass-transfer is dominant and rate-controlling. The accounting and allocation of the losses associated with the various processes and by current density regimes is vital to the understanding and improvement of MEA performance. In each regime, the membrane-electrode interfacial structure plays an important role in determining cell performance. On/off cycle operation negatively impacts MEA, including gas diffusion layer and membrane-electrode interfacial structure, which may contribute to the loss of cell performance [19]. By comparing performance curves carefully, a performance loss under RH 50% is observed slightly more than RH 80%.

Fig. 4 shows the impedance spectra of MEAs before and after on/off cyclic operation under different humid condition of RH 80% and RH 50%. Electrochemical impedance spectroscopy (EIS) is a powerful technique to characterize the resistance of a membrane and an electrode-electrolyte interface. The impedance response of

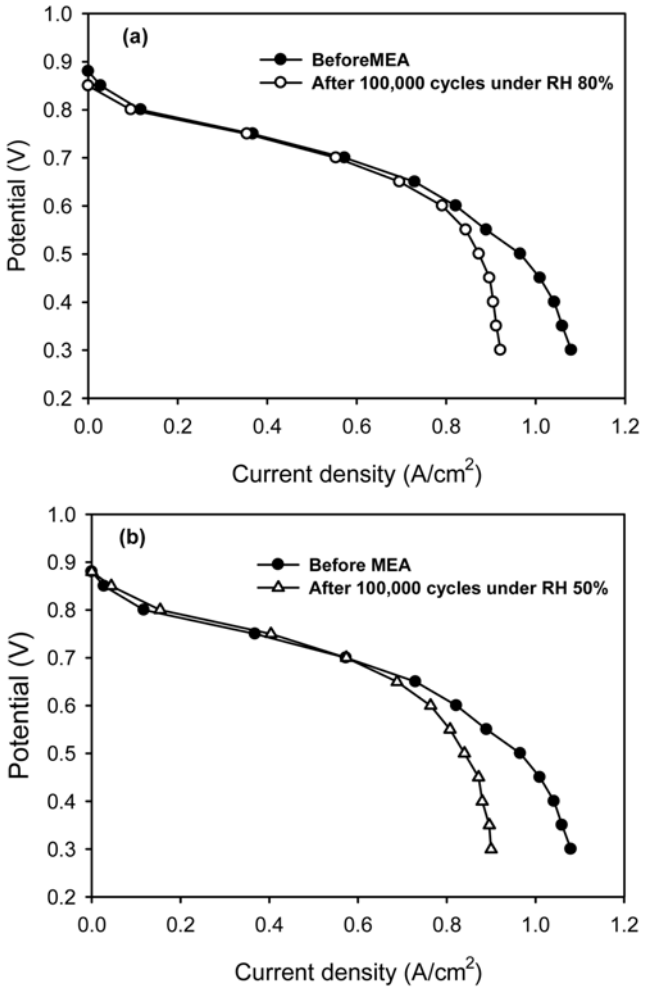

Fig. 3. Fuel cell performance for the MEAs before and after on/off operation for 100,000 cycles (a) under humid condition of RH 80%, and (b) under humid condition of RH 50%. The cell temperatures are at 70 °C and operating on H_2/air at 1/1 atm with fully humidification.

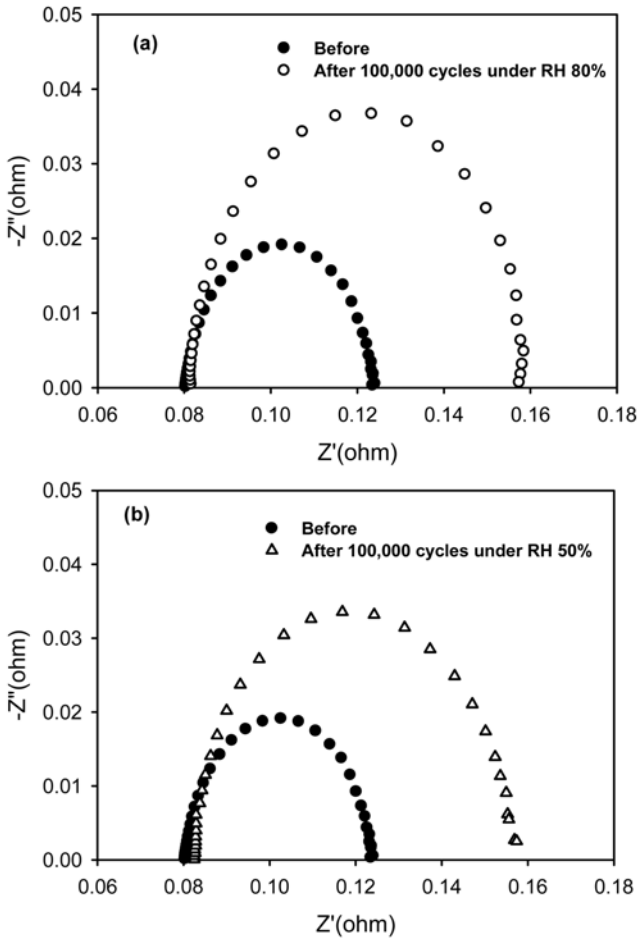

Fig. 4. Impedance spectra for the MEAs before and after operating 100,000 cycles (a) under RH 80%, and (b) under RH 50%. The anode and cathode were fed with fully humidified H_2/air of flow rate 100 sccm/ 500 sccm at 70 °C cell temperature. Measurements were carried out with two electrode ac impedance technique, frequency range from 10 kHz to 0.1 Hz, amplitude at 10 mV, and cell potential at 0.8 V.

an H_2/air PEM fuel cell will change along the I-V curve, depending on which loss processes are dominant. At higher currents, the impedance behavior is influenced by mass transport effects with decreasing the activation impedance loop. At low current, the activation kinetics dominate and the polarization resistance (R_p) is large, while the mass transport effects can be neglected [20]. Furthermore, the impedance spectrum measured at high cell voltage above 0.75 V (low current) typically consists of a single semicircle with the high frequency intercept point corresponding to the ohmic resistance of the membrane, and a diameter corresponding to the polarization resistance (R_p) including charge transfer resistance and diffusion resistance [21-23]. In our experiment, the in situ recorded impedance spectra were implemented at 0.8 V, which may give some important information on the ageing of the various MEA components. The membrane resistances before and after on/off cycles are similar values of about 0.08 Ω. These values are nearly constant, which indicates that the membrane resistances may not be affected during on/off operation for 100,000 cycles. On the other hand, the polarization resistances are dramatically increased from 0.04 Ω to 0.08 Ω for both humid condition of 80% and 50% similarly. These results indicate that on/off cyclic operation may contribute to the change in interfacial property between membrane and electrode.

Cyclic voltammetry (CV) is used to assess the electrochemical area (ECA) of electrodes. The ECA of Pt catalyst in a fuel cell cathode can be calculated based on the relationship between surface area and the charge associated with hydrogen adsorption on the electrode. The hydrogen adsorption charge on a Pt electrode is 210 μC/cm^2-Pt. The area of the hydrogen adsorption peaks gives us a quantitative measure of the area of Pt electrochemically available [24]. Fig. 5 shows a comparison of cyclic voltammograms for the MEAs before and after on/off cycles. Hydrogen adsorption peaks after 100,000 cycles both RH 80% and RH 50% at 0-3.5 V exhibit a similar transformation of their profiles, roughly overlapping, with decreasing the area of hydrogen adsorption peak about 6% than before on/off cyclic operation. These results confirm that the electrochemical area of MEA is little affected by on/off cyclic operation. The PtO reduction peak around 0.7 V shifts slightly to high potentials and decreases in intensity, which may be attributed to the increase of particle size

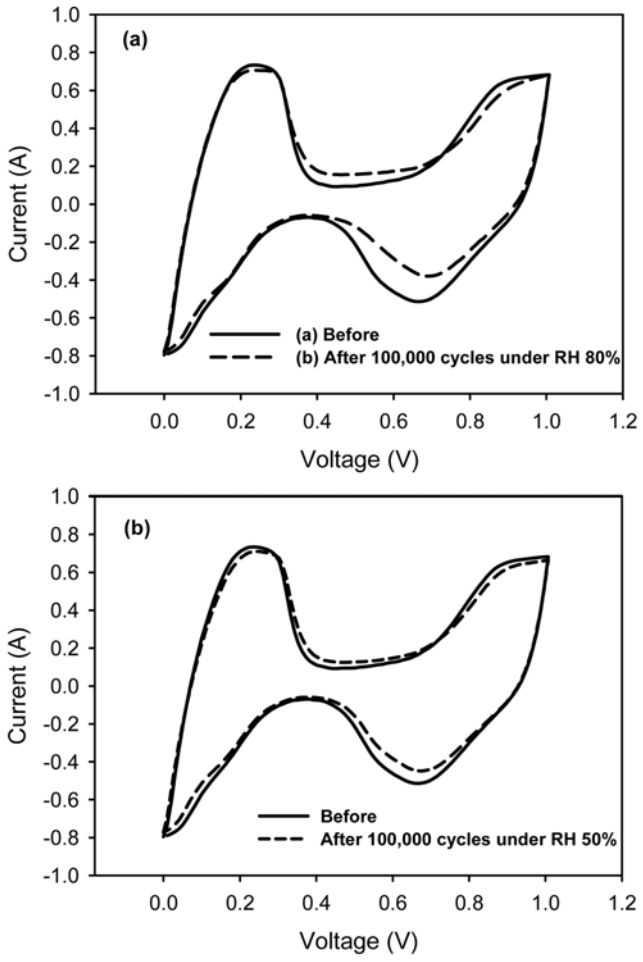

Fig. 5. Cyclic voltammograms for the MEAs before and after operating 100,000 cycles (a) under RH 80%, and (b) under RH 50%. All curves were measured at 70 °C with 200 sccm H_2 at the anode, and 200 sccm N_2 at the cathode. For CV, the sweep rate was 0.1 V/s and the the cell was cycled between 0.0 V and 1.0 V.

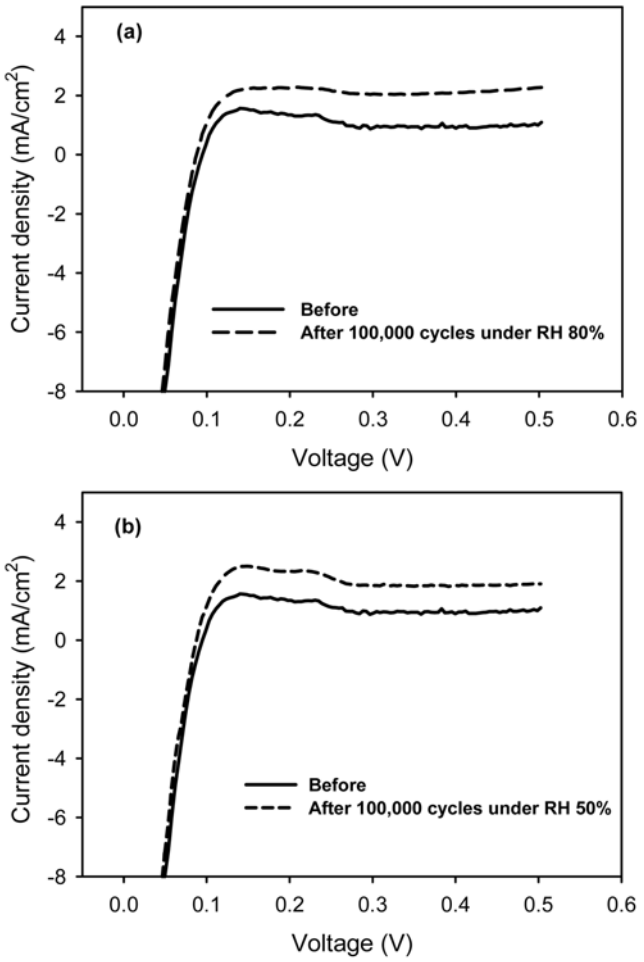

Fig. 6. Linear sweep voltammetry for the MEAs before and after operating 100,000 cycles (a) under RH 80%, and (b) under RH 50%. All curves were measured at 70 °C with 200 sccm H_2 at the anode, and 200 sccm N_2 at the cathode. For LSV, the sweep rate was 4 mV/s and the the cell potential was scanned from 0.0 V and 0.5 V.

by sintering [9].

Fig. 6 shows the limiting hydrogen crossover currents for the MEAs before and after on/off cycles by using linear sweep voltammetry (LSV). Crossover hydrogen current is related to quantify the hydrogen crossover through the membrane. Hydrogen that crosses over to the cathode is oxidized by the applied voltage at 0.35-0.5 V, and the measured current corresponds to the oxidation of the hydrogen molecules at the cathode side in the presence of platinum catalyst. Proton exchange membranes usually exhibit a small crossover of hydrogen gas from the anode to the cathode. If the hydrogen crossover rate from the anode to cathode increases dramatically, it is usually assumed that macroscopic pinholes have formed in the membrane [25]. The H_2 crossover currents of MEAs before and after 100,000 cycles under RH 80% and RH 50% were obtained with 1.0, 2.0, and 1.8 mA/cm^2. These results suggest that the membrane is slightly affected by the MEA physical degradation during the on/off cycles.

To help identify the cause of electrocatalyst surface area loss, XRD was used to measure the particle size of Pt. Fig. 7 shows XRD patterns for fresh MEA and MEAs after on/off operation for 100,000 cycles, both under RH 80% and RH 50%. The average platinum crystal sizes for the anode and the cathode were estimated from X-ray diffraction patterns using full-width at half maximum of the Pt (111) peak around 38° and summarized in Table 1. Pt particle size of the fresh MEA was found to have a 2.53 nm at anode and cathode, respectively. After on/off cycles, Pt particle size of anode increased to 3.79 and 3.78 nm under RH 80% and RH 50%, and that of cathode increased to 2.93 and 3.47 nm under RH 80% and RH 50%. The growth in electrocatalyst particle size is related to the loss in electrocatalyst surface area. In addition, the relative humidity was observed to have an effect on the growth of platinum particles. The platinum particle size is increased larger under higher humid condition of RH 80% than RH 50% during on/off operation, which may be related to the lowered activation energy of particle growth [10].

Pt line profiles for the MEAs were performed by EDX analyses and the results are presented in Fig. 8. The decreases of Pt peaks are observed at the cross-section of MEAs operated 100,000 cycles under RH 80% and RH 50%. These results suggest that the losses

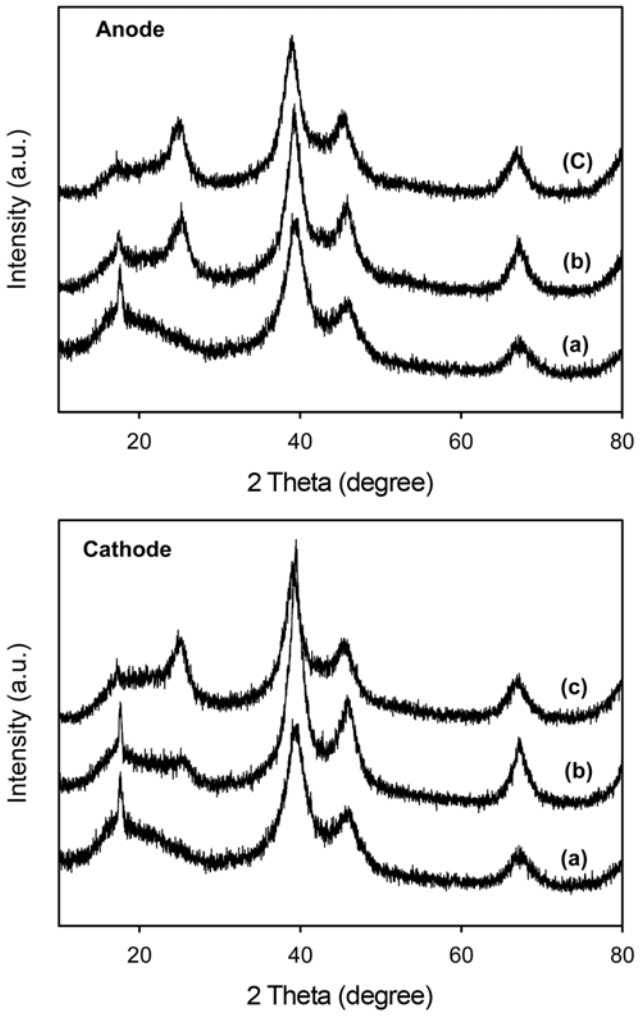

Fig. 7. X-ray diffraction pattern of (a) the fresh MEA, (b) after the MEA operated 100,000 cycles under RH 80%, and (c) the MEA operated 100,000 cycles under RH 50%.

Table 1. The size of Pt particles calculated from X-ray patterns. The particle size was measured by the Pt (111) peak

MEAs	Anode (nm)	Cathode (nm)
Fresh	2.53	2.53
After 100,000cycles under RH 80%	3.79	3.78
After 100,000cycles under RH 50%	2.93	3.47

of platinum catalyst occurred by on/off operation quantitatively. Moreover, Pt peak is not observed in the membrane during physical degradation.

CONCLUSIONS

Assessments of the physical degradation of MEAs in the PEM fuel cell were provided by on/off cyclic operation with N_2/N_2. After on/off operation for 100,000 cycles, performance drops were observed at high current density in both humid conditions of RH 80% and RH 50%, which may be due to the degradation of the membrane-electrode interfacial structures. In our experiments, the membrane resistance was constant while the polarization resistance was from 0.04 Ω to 0.08 Ω under two different humid conditions similarly. The electrochemical area and the hydrogen crossover current were slightly affected by on/off cycle operation. The results of XRD analyses indicated that the size of the Pt catalyst increased during on/off operation, and the rate of Pt particle growth was greater under high relative humidity.

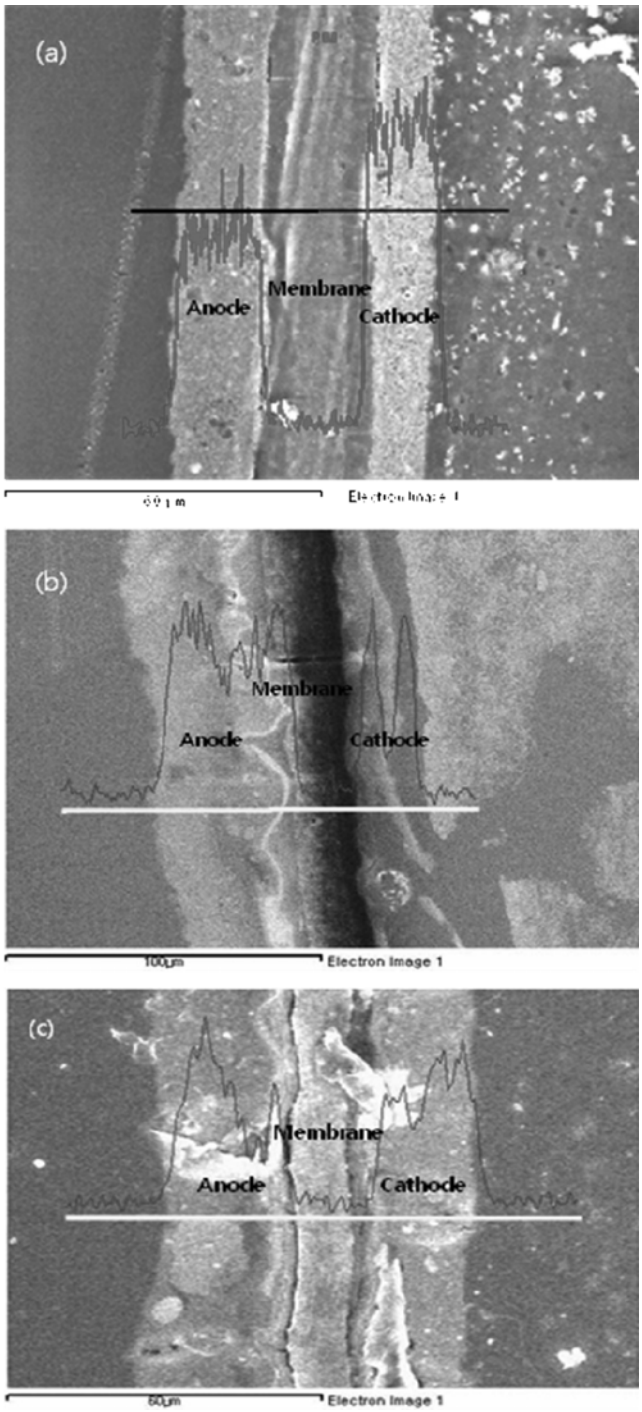

Fig. 8. EDX images and Pt line scanning of (a) the fresh MEA, (b) after the MEA operated 100,000 cycles under RH 80%, and (c) after the MEA operated 100,000 cycles under RH 50%.

ACKNOWLEDGEMENT

This work was supported by Brain Korea 21 and the fostering project of the Specialized Graduate School of Hydrogen & Fuel Cell supported financially by the Ministry of Commerce Industry and Energy (MOCIE).

REFERENCES

1. R .S .Gemmen and C. D. Johnson, *Journal of Power Sources*, **159**, 646 (2006).
2. W. Schmittinger and A. Vahidi, *Journal of Power Sources*, **180**, 1 (2008).
3. M. Marrony, R. Barrera, S. Quenet, S. Ginocchio, L. Montelatici and A. Aslanides, *Journal of Power Sources*, **182**, 469 (2008).
4. D. Liu and S. Case, *Journal of Power Sources*, **162**, 521 (2006).
5. S. Zhang, X. Yuan, H. Wang, W. Mérida, H. Zhu, J. Shen, S. Wu and J. Zhang, *International Journal of Hydrogen Energy*, **34**, 388 (2009).
6. A. Taniguchi, T. Akita, K. Yasuda and Y. Miyazaki, *International Journal of Hydrogen Energy*, **33**, 2323 (2008).
7. P. J. Ferreira, G. J. la O', Y. Shao-Horn, D. Morgan, R. Makharia, S. Kocha and H. A. Gasteiger, *Journal of The Electrochemical Society*, **152**(11), A2256 (2005).
8. D. A. Stevens, M. T. Hicks, G. M. Haugen and J. R. Dahn, *Journal of the Electrochemical Society*, **152**(12), A2309 (2005).
9. A. S. Aricó, A. Stassi, E. Modica, R. Ornelas, I. Gatto, E. Passalacqua and V. Antonucci, *Journal of Power Sources*, **178**, 525 (2008).
10. R. L. Borup, J. R. Davey, F. H. Garzon, D. L. Wood and M. A. Inbody, *Journal of Power Sources*, **163**, 76 (2006).
11. S. Maass, F. Finsterwalder, G. Frank, R. Hartmann and C. Merten, *Journal of Power Sources*, **176**, 444 (2008).
12. H. Tang, Z. Qi, M. Ramani and J. F. Elter, *Journal of Power Sources*, **158**, 1306 (2006).
13. O. A. Baturina, S. R. Aubuchon and K. J. Wynne, *Chemistry Material*, **18**, 1498 (2006).
14. A. B. Laconti, M. Hanmada and R. C. Mcdonald, *Handbook of fuel cells-fundamentals, technology, and application*, Wiley & Sons, Ltd., Chapter 49, 647 (2003).
15 S. Sugawara, T. Maruyama, Y. Nagahara, S. S. Kocha, K. Shinohra, K. Tsujita, S. Mitsushima and K. Ota, *Journal of Power Sources*, **187**, 324 (2009).
16. V. O. Mittal, H. R. Kunz and J. H. Fenton, *Journal of the Electrochemical Society*, **153**(9), A1755 (2006).
17. A. Collier, H. Wang, X. Z. Yuan, J. Zhang and D. P. Wilkinson, *International Journal of Hydrogen Energy*, **31**, 1838 (2006).
18. J. Wu, X. Z. Yuan, J. J. Martin, H. Wang, J. Zhang, J. Shen, S. Wu and W. Merida, *Journal of Power Sources*, **184**, 104 (2008).
19. S. S. Kocha, *Handbook of fuel cells-fundamentals, technology, and application*, Wiley & Sons, Ltd., Chapter 43, 538 (2003).
20. R. O'Hayre, S.-W. Cha, W. Colella and F. B. Prinz, *Fuel cell fundamentals*, John Wiley & Sons, Ltd. (2006).
21. M.Ciureanu and R. Roberge, *Journal of Physical Chemistry B*, **105**, 3531 (2001).
22. C. S. Kong, D.-Y. Kim, H.-K. Lee, Y.-G. Shul and T.-H. Lee, *Journal of Power Sources*, **108**, 185 (2002).
23. B. Wahdame, D. Candusso, X. Francois, F. Harel, M.-C. Pera, D. Hissel and J.-M. Kauffmann, *International Journal of Hydrogen Energy*, **32**, 4523 (2007).
24. T. R. Ralph, G. A. Hards, J. E. Keating, S. A. Campbell, D. P. Wilkinson, M. Davis, J. St-Pierre and M. C. Johnson, *Journal of the Electrochemical Society*, **144**, 3845 (1997).
25. Z. Zhang, Z. Xie, J. Zhang, Y. Tang, C. Song, T. Navessin, Z. Shi, D. Song, H. Wang, D. P. Wilkinson, Z.-S. Liu and S. Holdcroft, *Journal of Power Sources*, **160**, 872 (2006).